Site-Specific Deposition of Au Nanoparticles in CNT Films by Chemical Bonding

Aruna Velamakanni,[†] Carl W. Magnuson,[‡] K. J. Ganesh,[‡] Yanwu Zhu,[†] Jinho An,[†] Paulo J. Ferreira,[†] and Rodney S. Ruoff[†,*]

[†]Department of Mechanical Engineering and The Texas Materials Institute and [‡]Materials Science and Engineering Program, The University of Texas at Austin, 1 University Station, C2200, Austin, Texas 78712-0292

T he overall electrical, thermal, and mechanical performance of networks of overlapped and crisscrossed carbon nanotubes (CNTs) (also called buckytube paper, CNT films, *etc.*) is largely determined by the nature of the contact at the node—that is, the intersection of overlapping CNTs. To our knowledge, there has been no work to date on selective modification of the nodes in CNT networks, and we report here on such an effort, with an eye towards improving the transparent electrode performance of such networks.

Transparent electrical conductors are a key component in modern technology, used in various applications[1,8,9] including, but not limited to, solar cells, flat panel displays, solid state lighting, still-image recorders, lasers, optical communication devices, electrodes in flexible electronics, and sensitive bolometers for detecting infrared radiation. Transparent conductive films (TCFs) based on CNTs are a promising candidate for potential use in all of the above applications and have been touted as a possible replacement for the currently used indium tin oxide (ITO) films. CNT films could offer a lower cost solution that is far more compatible with high volume production techniques, and, unlike metal oxide films, CNT films can be deposited with high volume roll-to-roll processes. CNT films are far more compliant than brittle metal oxide films, suggesting their use in plastic electronics and solar cells, thus offering interesting possibilities for both fundamental science and important technological areas. Random or quasi-random networks of CNTs ("CNT nets") have been made in thin film form and studied for use in applications such as those mentioned above.[1,8,9]

ABSTRACT There has been no attempt to date to specifically modify the nodes in carbon nanotube (CNT) networks. If the nodes can be modified in favorable ways, the electrical and/or thermal and/or mechanical properties of the CNT networks could be improved. In an attempt to influence the performance as a transparent conductive film, gold nanoparticles capped with the amino acid cysteine (Au-CysNP) have been selectively attached at the nodes of multiwalled carbon nanotubes (MWCNTs) networks. These nanoparticles have an average diameter of 5 nm as observed by TEM. FTIR and XPS were used to characterize each step of the MWCNT chemical functionalization process. The chemical process was designed to favor selective attachment at the nodes and not the segments in the CNT networks. The chemical processing was designed to direct formation of nodes where the gold nanoparticles are. The nanoparticles which were loosely held in the CNT network could be easily washed away by solvents, while those bound chemically remained. TEM results show that the Cys-AuNPs are preferentially located at the nodes of the CNT networks when compared to the segments. These nanoparticles at the nodes were also characterized by a novel technique called diffraction scanning transmission electron microscopy (D-STEM) confirming their identity. Four-probe measurements found that the sheet resistance of the modified CNT networks was half that of similarly transparent pristine multiwalled CNT networks.

KEYWORDS: transparent conductive film · multiwalled carbon nanotube · cysteine-capped gold nanoparticle · D-STEM

However, application of CNT networks as thin films for TCFs has a major limitation, their relatively high electrical resistance. If the electrical conductivity of CNT nets could be significantly improved, the technological value of these thin films as transparent conductive electrodes would be enormously improved. The overall electrical resistance of CNT based TCFs is largely determined by the resistance at the crossing points (also called nodes or junctions) of the CNTs. We define the CNT network as being composed of nodes and segments. Modeling studies of networks of one-dimensional elements have shown a resistivity dependence on segment length distributions and node resistances.[2] The electrical resistance at the nodes of CNT networks has been estimated through Monte Carlo modeling to be approximately 100 times larger than the quantum resistance of
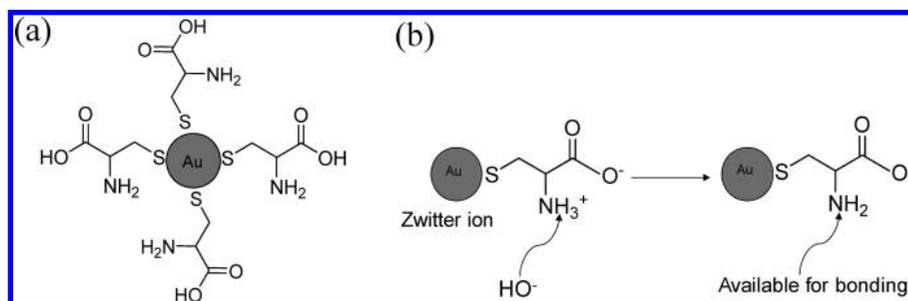
Figure 1. (a) Schematic depicting the attachment of cysteine molecules to make Au-Cys nanoparticles. **(b)** Schematic showing the availability of the $-NH_2$ group for bonding upon changing the pH by addition of base (OH^-) ions.

6.5 kΩ—as determined by fitting experimental $I-V$ data of actual CNT nets.[3] Through such modeling, it has been shown that, if the node resistance value were identical to the quantum resistance, the overall CNT net resistance could be lowered by about a factor of 10.[3] So, for the specific types of networks that have been modeled, improvements up to a factor of 10 could, in principle, be achieved if the node resistance were markedly lower.[4] The nature of the bonding at the node also plays a central role in the mechanics of CNT nets, per modeling studies.[5,6] For example, replacing the weak van der Waals contact of two crossing CNTs with strong covalent bonds could significantly improve the mechanical performance, and such a CNT net would be sufficiently robust[7] to be infiltrated with other materials such as polymers, ceramics, and perhaps even metals. The robust CNT net could then serve in structural applications and would further be capable of being an electrically and thermally conductive component in, for example, insulating matrix materials, with potential use in smart material applications.

We present a chemical approach for "selectively depositing" functionalized gold nanoparticles at the nodes of multiwalled carbon nanotubes (MWCNTs). Previous work which incorporated gold nanoparticles into MWCNT networks did not target the selective deposition of nanoparticles at the nodes of the networks. Methods that lead to a random distribution of gold nanoparticles include solution-based,[10–15] electrostatic,[16] gold evaporation,[17,18] and γ-radiation.[19] Here we have demonstrated control on the deposition of gold nanoparticles capped with cysteine (Au-Cys, Figure 1a) at the nodes of MWCNT networks. The main goal of this work is to explore the fundamental science of a method for selective deposition of material at the nodes of MWCNT networks. Following the procedure of chemical linking and annealing, we have ensured that we have conductive material (gold nanoparticles) deposited specifically at the nodes and not randomly on the MWCNT films. This will potentially enhance the performance of TCFs based on MWCNTs, and the endeavor of achieving selective deposition at the nodes will hopefully inspire others to find routes to achieving this as well.

RESULTS AND DISCUSSION

Cysteine is an amino acid with three functional groups: thiol ($-SH$), amino ($-NH_2$), and carboxylic acid ($-COOH$). While the $-SH$ group interacts with the gold nanoparticle *via* the gold–thiol bond, the $-NH_2$ and $-COOH$ groups can make chemical bonds with the complementary groups on functionalized MWCNTs. Cysteine at pH 7 is a zwitterion and thus has positive and negative charges on different atoms in the molecule but a net zero overall charge. Specifically, the $-NH_2$ and $-COOH$ groups exist as $-NH_3^+$ and $-COO^-$ due to migration of a proton from the $-COOH$ group to the $-NH_2$ group. However, the pH can be adjusted such that one of those groups can be made available for reaction. In the present work, we have added a weak base, ammonium hydroxide (NH_4OH), to adjust the pH to 10 so as to react with the conjugate acid NH_3^+. Thus, NH_3^+ is converted back to a free amino ($-NH_2$) group that is then available for reaction with the acid chloride ($CO-Cl$) groups (obtained after multiple steps of functionalization; details in Methods section) on the MWCNTs. A schematic of this is shown in Figure 1b. When one cysteine-capped gold nanoparticle (Au-CysNP) gets linked to a MWCNT chemically, the remaining groups on the same Au-CysNP can link to other MWCNTs. This results in a gold nanoparticle "drawing" two (or more in some cases) MWCNTs together and "trapping" itself at the resulting intersection or the node of the two MWCNTs. Some Au-CysNPs are not able to link with other MWCNTs and remain at places other than the nodes such as the segments or the end caps of MWCNTs (see Supporting Information). It is well-known that gold strongly dewets from certain types of CNTs,[20] thereby tending to minimize their ability to aid in the electrical contacts between tubes. However, the morphological stability of the gold film/nanoparticles depends on the relative strength of the interface bonds (adhesion),[21] and in the present case, gold nanoparticles are chemically bound to the MWCNTs and hence are more strongly attached than if they were physically adsorbed. Annealing these films at 400 °C for an hour leads to the decomposition of cysteine into various gaseous products, leaving just the gold nanoparticles at the nodes. The strong covalent bonds by which they were originally attached to the MWCNTs help them re-

main at the same position even after annealing and losing the cysteine capping; it has been reported that pure cysteine thermally decomposes at 400 °C.[22] TEM images (see Supporting Information Figure S11) after annealing show that the gold nanoparticles do not dewet and are still located at the network nodes.

Control experiments were conducted where the gold nanoparticles were not capped with cysteine to observe if there was still specificity in linking of the gold nanoparticles. Films were made with these non-cysteine-capped gold nanoparticles following the same procedure used for MWCNT-Au-CysNPs. It was found that the gold nanoparticles agglomerated to larger particles and most of the gold nanoparticles simply did not adhere to the MWCNTs. (TEM and SEM images of networks with Au nanoparticles not capped with cysteine can be found in the Supporting Information.) The very few nanoparticles that did stay within the network were located randomly on the network as opposed to what was found when they were capped. We attribute this to the lack of cysteine capping around the gold nanoparticles, which not only stabilized them and prevented agglomeration but also provided complementary groups ($-NH_2$ with $-COCl$) to bond with the functionalized MWCNTs. The Au-CysNPs were first linked to the tubes, and then the films were made. This procedure ensures that the location of gold nanoparticles on MWCNTs is due to the chemical bonds and that they are thus located at positions where they are linking the tubes. When a film is made with such linked tubes, the gold nanoparticles remain at the intersections of the tubes. These intersections are (some of) the nodes of the CNT networks/films. However, if a film is first made and then the gold nanoparticles are deposited, there is very little control on directing the nanoparticles to the junctions, resulting in a random dispersion across the network as evidenced by the TEM results. This remains an exciting challenge for future work-selective deposition at the nodes of already-made CNT nets.

A phase contrast image of a sparse MWCNT-Au-CysNP network is seen in Figure 2a. Four different samples were observed, and 150 nodes in each sample were analyzed. It was observed that 85% of the particles were at the nodes and the remaining 15% were along the segments. Also many nodes were unoccupied by Au-Cys particles, leaving them as unmodified nodes. Figure 2b shows a high magnification TEM image of a Au-CysNPs between two MWCNTs. TEM was also used to examine areas of the MWCNT networks that were sparse enough to clearly differentiate between network nodes and segments. Measurement of the linear lengths of the segments and nodes showed that 30% of the overall lengths of the MWCNTs were located at nodes (see Supporting Information for additional details on how this was measured). However, in these areas, 85% of the gold nanoparticles were located at the

nodes. If the particles were randomly distributed along the MWCNTs, one would expect only 30% to be at the nodes. This clearly shows that the Au-CysNPs are more selectively deposited at the network nodes.

Using the same TEM sample as in Figure 2a, a line scan using micro-EDS across a gold nanoparticle (~5 nm in diameter) located at a node of the MWCNT network revealed that the nanoparticle was coated with a thin layer of sulfur (Figure 2b inset), which is due to the gold−thiol linkage. This has also been proven by XPS data as discussed below.

A recently developed technique called D-STEM was also employed to identify the material deposited at the nodes. Our interest was to characterize just the nanoparticle at the node and not the surrounding material in order to confirm that the material deposited at the node was in fact a gold nanoparticle. The nano-beam diffraction (NBD) technique was not used to characterize the material at the nodes in spite of having a very small beam size because, during operation, the NBD technique requires constant toggling between the image and diffraction modes, which might result in potential beam shifts, thereby affecting position accuracy. In D-STEM, the enhanced control and precise positioning of the beam on the region of interest enables rapid collection of sharp spot patterns from nanostructures as small as 3 nm. The details of this technique can be found elsewhere.[23,24] Figure 2c shows a representative bright-field STEM image of nodes with nanoparticles (details on the resolution of this image can be found in the Supporting Information). The 1−2 nm diameter near-parallel probe was positioned on the nanoparticle labeled (A), and the diffraction pattern obtained is shown in Figure 2d. The obtained four-fold diffraction pattern was indexed to a [001] beam direction and, when compared, the inter-planar spacings revealed a perfect match to gold (Au(0)). A single-crystal Si [110] specimen was used to calibrate the camera length for this technique.

Figure 3a shows the XPS survey spectra of unannealed and annealed films deposited on glass. The survey spectrum of unannealed film showed peaks for sulfur and nitrogen in addition to gold, carbon, and oxygen. A better insight into the binding of the Au-CysNPs was obtained by looking at the high resolution elemental spectra of the individual elements present. Figure 3b shows the C 1s peak for the MWCNT-Au-Cys films before annealing. This was fit to four components: the component at 288.0 eV corresponds to amide linkage ($-NH-C\equiv O$), 285.8 eV to $-C-O$ in hydroxyl groups (which get incorporated during oxidation along with the carboxylic groups), and the remaining two peaks at 284.5 and 284.7 eV to the sp^2 and sp^3 carbons, respectively, in MWCNTs. Figure 3c shows the C 1s peak for the annealed Au-Cys-MWCNT films. The peaks at 284.5 and 284.8 eV correspond to the sp^2 and sp^3 carbons, respectively, in the MWCNTs. The peak at 286.4 eV corresponds to the $-C-OH$, which remains af-
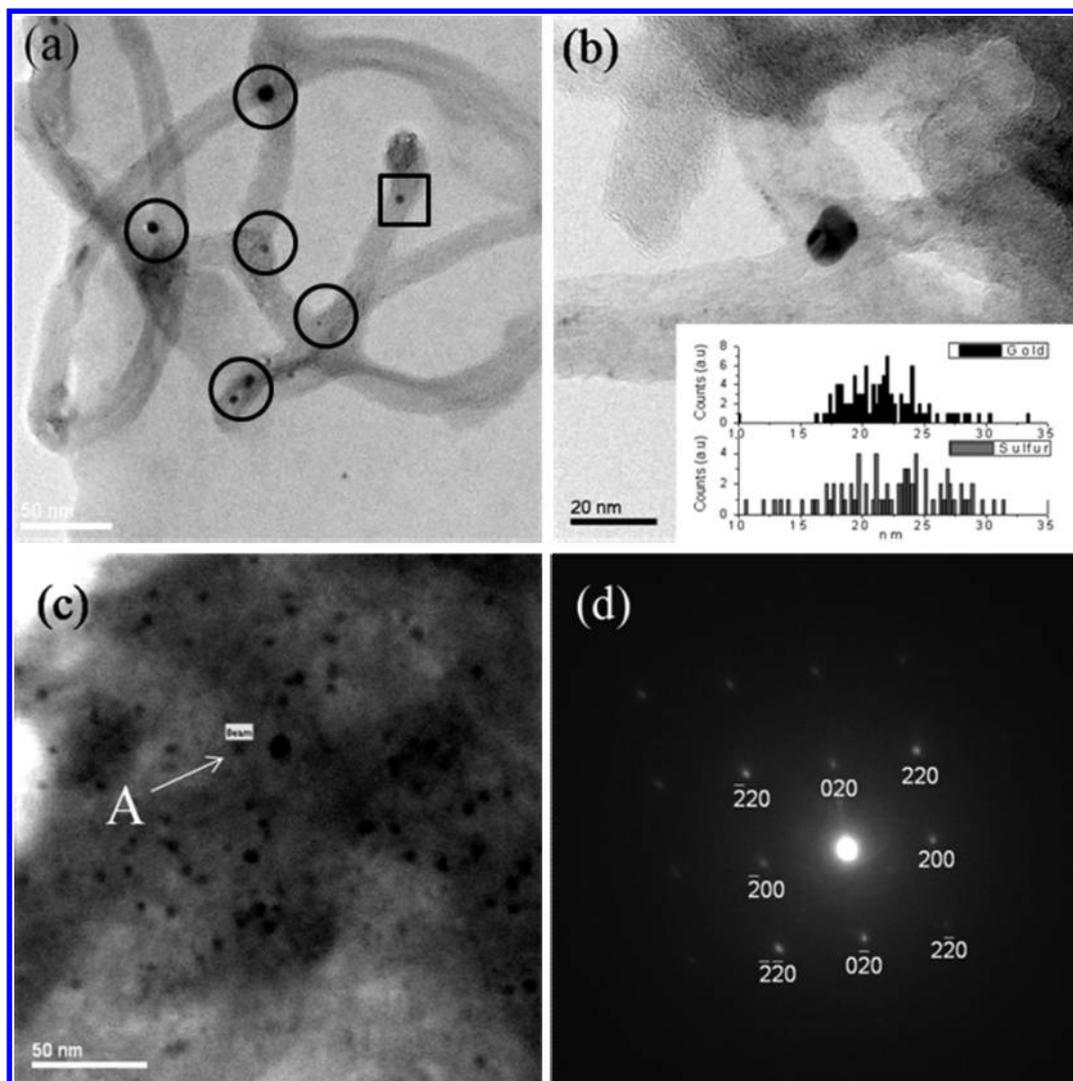
Figure 2. (a) Bright-field TEM micrograph of the MWCNT network showing Au-Cys nanoparticles at the nodes (circled) and one along a segment (squared). (b) High magnification phase contrast image of one of the nodes. Inset: Micro-EDS line profile for gold and sulfur across the Au-Cys nanoparticle. (c) Bright-field STEM image of the MWCNT network showing the D-STEM beam positioned exactly at one of the Au-Cys nanoparticles labeled A. (d) Spot diffraction pattern obtained by D-STEM from the nanoparticle shown in (c). The bright center spot in the diffraction pattern is (000).

ter annealing. It was observed that the other high oxidization peaks disappear, such as the amide in the previous case. Instead, a shakeup peak at 290.2 eV appears. The shakeup peaks which are due to $\pi-\pi^*$ transitions are more pronounced in the conjugated and aromatic systems and occur above 290 eV.[25,26] In the case of functionalized tubes with Au-CysNPs, the conjugation is largely disrupted by the introduction of sp^3 carbons due to oxidation and chemical bonding. After annealing when the cysteine capping is decomposed (loss of amide bonds) and more sp^2 bonding is attained due to decarboxylation of the MWCNTs, the shakeup peak became more prominent, as seen in Figure 3c. The origin of the N 1s peak at 400.5 eV (Figure 3d) is due to the incorporation of the amide bond that is formed by linking the Au-CysNPs to the MWCNTs. A peak corresponding to the amide bond is also seen in the C 1s spectrum at 288.0 eV. The S 2p peak was deconvolved into two components for the unbound thiol due to any free cys-

teine at 164.1 eV and another peak at 162.5 eV[27−30] due to the gold−thiol interactions. Both the N 1s and S 2p peaks disappeared completely in the annealed films. This is attributed to the decomposition of cysteine into various gaseous products at 400 °C.[22] Figure 3f shows the comparative spectra of Au 4f before and after annealing. The Au 4f (7/2) peak has been referenced at 84 eV, which is typical of Au(0).[31,32] The Cl 2p peak is absent in both the annealed and unannealed films, confirming the absence of AuCl$_3$. This eliminated the possibility of other species such as Au^{3+} that might also contribute to the signal for Au in XPS. Indexing the D-STEM diffraction pattern from the particles at the nodes proved that these particles are Au(0) and not a compound such as AuCl$_3$ containing Au^{3+}. Hence it can be concluded that Au^{3+} is not present, and the signal for gold is, in fact, coming from Au(0). The incorporation of −Cl in the form of −CO−Cl in the MWCNTs (see Supporting Information) and attachment of the Au-
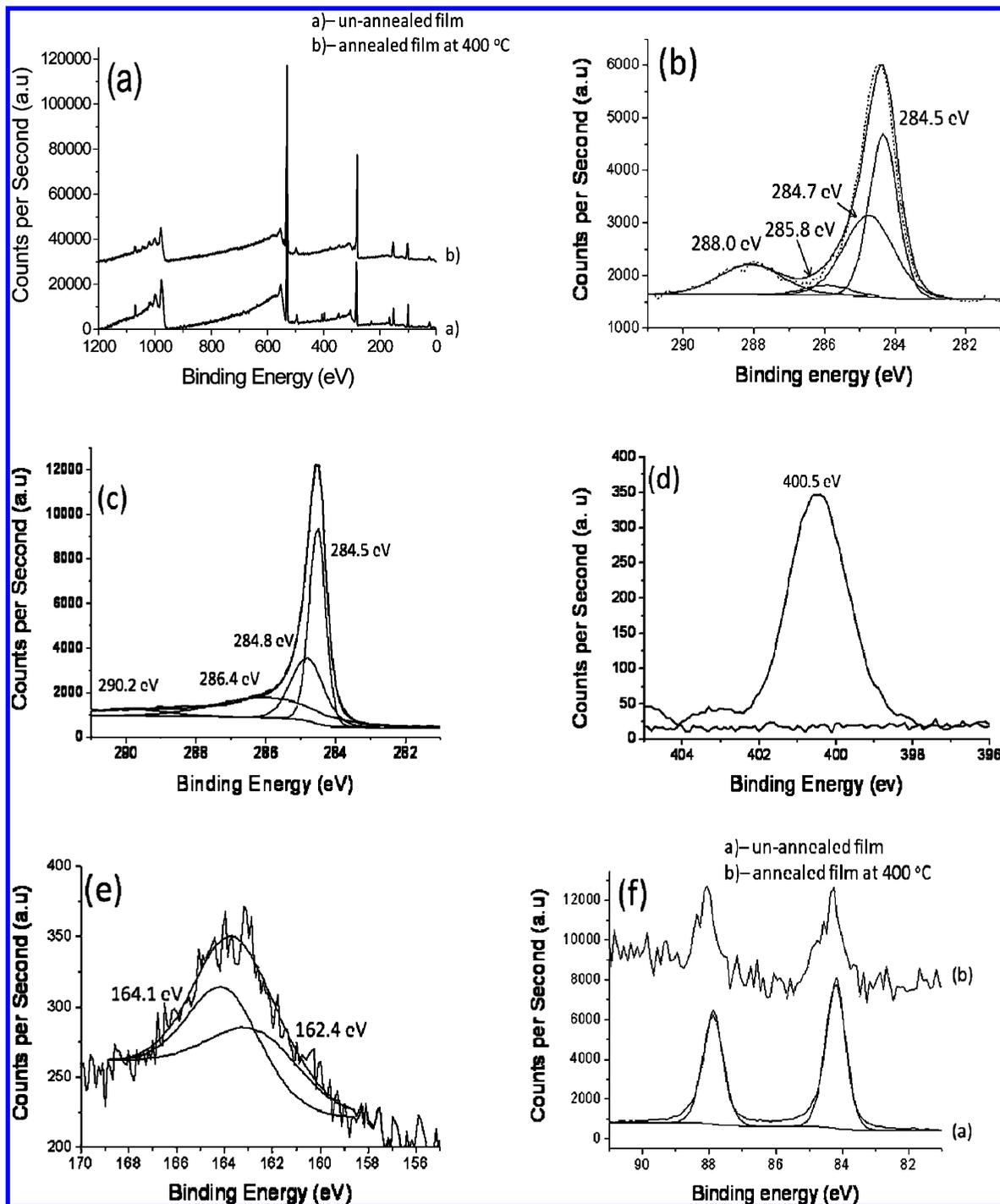
Figure 3. (a) XPS survey scan of MWCNT-Au-Cys films before and after annealing. The peaks corresponding to nitrogen and sulfur disappear after annealing. (b) Deconvolved C 1s peak for the unannealed film. (c) Deconvolved C 1s peak for the annealed film. (d) N 1s peak (400.5 eV) before annealing; disappears after annealing. (e) Deconvolved S 2p peak. (f) Au 4f peaks are present both before and after annealing.

CysNPs to the MWCNTs have been successfully proven by XPS; this was otherwise very difficult by FTIR due to the limit of detection for that technique, owing to the fact that mild oxidation was used and so fewer functional groups were introduced.

The van der Pauw four-probe method[33] was used to measure (Keithley 6221 and 6514) the sheet resistivity of the vacuum-filtered films after they were transferred onto glass substrates. The resistivity of four films

from the same mixed cellulose ester (MCE) membrane before annealing was ~580 kΩ/□. After annealing under argon at 400 °C for 1 h, the resistivity of the thin conductive films dropped to 19.5 kΩ/□. The transmittances of the same films (Figure S8 in the Supporting Information) measured at 550 nm with a spectroscopic ellipsometer (J. A. Woollam M2000D) were found to be 54.8 ± 0.3%. Four TCFs made with pristine MWCNTs from the same MCE membrane with transmittance 53.1 ±

0.2% were found to have a sheet resistance of 41 kΩ/□. Even though the pristine MWCNT TCFs were slightly less transparent than the modified films, their sheet resistance was over twice as large. Annealing the TCFs for 1 h at 400 °C under argon did not change their transmittance nor did it change the sheet resistance of the pristine MWCNT films. (I−V curves of all three types of films can be found in Figure S9 of the Supporting Information.)

CONCLUSIONS

Au-CysNPs were incorporated selectively at the nodes of CNT networks. These nanoparticles are chemically bound to the MWCNTs *via* amide bonds and are preferentially located at the nodes of the MWCNT network rather than along the segments. Since the weak van der Waals contact of two crossed CNTs has been successfully replaced by strong covalent bonds, the mechanical performance of the CNT net might also be improved and is thus suggested as a topic of further study.

The electrical resistivity of TCFs made with MWCNT-Au-Cys is roughly half that of those with the same transmittance but composed of pristine MWCNTs alone. This is the first report of an experimental attempt to selectively modify the nodes and not the segments of CNT networks so as to enhance the performance of such networks. The concept of selective modification of the nodes in CNT networks is a topic of a recent patent filing by one of the authors.[34] A recent publication (appearing after our submission of the work presented here) by Rodríguez-Manzo *et al.*[35] explored irradiating a cobalt nanoparticle located near the node of two MWCNTs to "nano-weld" the MWCNTs together, with a focused electron beam in a TEM at elevated temperatures. Combining the selective deposition of nanoparticles at the nodes of MWCNT networks, as shown in the current work, with nano-welding of nanoparticles attached to the MWCNTs *en masse* by large area irradiation is suggested for future research.

METHODS

Acid-Functionalized MWCNTs (MWCNT-COOH): Multiwalled carbon nanotubes (Sigma Aldrich 99.97% pure 6−13 nm in diameter) were annealed at 225 °C for 24 h in air to remove any amorphous carbon and oxidize any catalyst particles. The annealed MWCNTs were then oxidized to generate −COOH functional groups by stirring with a mixture of concentrated sulfuric and nitric acid (3:1)[36] for 24 h. Stirring was used instead of sonication in an attempt to prevent the nanotubes from breaking at the end caps (Figure S5 in Supporting Information). The oxidized MWCNTs (MWCNT-COOH) were vacuum filtered (Millipore 1.0 μm PTFE) and thoroughly rinsed with deionized water (17.5 Mohms Barnstead).

Acid-Chloride-Functionalized MWCNTs (MWCNT-COCl): One hundred milligrams of MWCNT-COOH was stirred in 50 mL of thionyl chloride with 2 drops of dimethylformamide (DMF) as a catalyst, under argon for 24 h at 70 °C. The functionalized MWCNTs were vacuum filtered (Millipore 1.0 μm PTFE) and completely rinsed with tetrahydrofuran (THF) to prevent hydrolysis of the −COCl functional groups. The acid-chloride-functionalized MWCNTs (MWCNT-COCl) were stored under argon to prevent any hydrolysis and were used immediately for further reactions.

Synthesis of Gold Nanoparticles (Au-CysNPs): Cysteine-capped gold nanoparticles (Au-CysNPs) were prepared by a known method.[37] Briefly, reduction of tetrachloroauric acid with sodium borohydride, followed by addition of the amino acid cysteine, resulted in Au-CysNPs. The Au-CysNPs dispersed in water were purified to a diameter of 3−5 nm by centrifuging (IEC MediSpin) for 1 h. One milliliter of ammonium hydroxide was diluted with 100 mL of H_2O. The pH of 10 mL of Au-CysNPs was adjusted to 10.4 (measured with a Fisher Scientific Accumet Excel pH meter) by adding 6 drops of the diluted ammonium hydroxide.

Linking of Au-Cys with MWCNT-COCl (MWCNT-AU-CysNPs) and Making Films: Twenty milligrams of of MWCNT-COCl was suspended in 10 mL of THF, and 1 mL of the pH-adjusted Au-CysNPs was added dropwise while stirring under argon. The reactive −COCl groups on the MWCNT-COCl react with the free −NH₂ groups on the Au-CysNPs and are linked *via* an amide bond. The MWCNTs linked with Au-CysNPs (MWCNT-Au-Cys) were suspended in THF and stirred under argon for 2 days. The solution was then added to 190 mL of pure water. This hydrolyzed the remaining −COCl functional groups on the MWCNTs and created a good dispersion of the MWCNT-Au-CysNPs. After decanting the above solution, 6 mL of the supernatant was suspended in 200 mL of pure water and vacuum filtered onto a mixed cellulose ester (MCE) filter membrane (Sterlitech) and made into a thin film.[38] To obtain square films, each 47 mm diameter MCE membrane was cut into four smaller squares roughly 1 cm on a side. The film was transferred to a glass cover slide, and the MCE membrane was dissolved with acetone (soaked three times in an acetone bath for 20 min). After rinsing the thin conductive film with ethanol several times, which was observed to wash the unbound nanoparticles away, the film was annealed at 400 °C for 1 h under argon. The result is uncapped gold nanoparticles located at the nodes of the MWCNT network.

Characterization. The material was characterized after each step of modification to test whether the desired functionality was being introduced. A Perkin-Elmer UV−vis spectrophotometer in the range of 200−800 nm was used to monitor the UV−vis absorption spectra of free gold nanoparticles and the Au-CysNPs dispersed in water. Fourier transform infrared (FT-IR) spectroscopy (Supporting Information) and X-ray photoelectron spectroscopy (XPS) were used to follow the functionalization of MWCNTs at each step and also after linking them with the Au-CysNPs. XPS analysis was performed using a Kratos AXIS Ultra DLD XPS equipped with a 180° hemispherical energy analyzer to determine the chemical composition of these nanotubes. Photoemission was stimulated by monochromated Al Kα radiation (1486.6 eV) with an operating power of 150 W. It was operated in the analyzer mode at 80 eV for survey scans and 20 eV for detailed scans of core level lines. Binding energies were referenced to the C 1s binding energy set at 284.5 eV. After the Au-CysNPs were linked to the MWCNTs, TEM was done to observe the location of the particles. A drop of the suspension of MWCNT linked with Au-CysNPs was placed on a 400 mesh copper TEM Quantifoil holey carbon grid. This was investigated using a JEOL 2010F TEM/STEM (C_s = 0.5 mm) equipped with an ultrahigh resolution pole piece. An operating voltage of 200 kV was used. In STEM mode (0.5 nm probe, 15 cm camera length, 50 μm condenser aperture), micro-EDS determined if sulfur surrounded the gold nanoparticle *via* gold−thiol bond while in the MWCNT network. A recently developed technique called D-STEM (diffraction scanning transmission electron microscopy) was employed to confirm the identity of the particle at the node of two tubes.

Supporting Information Available: UV−vis spectra of the cysteine capped gold nanoparticles, FTIR spectra of functionalized MWCNTs (MWCNT-COOH, MWCNT-COCl), and MWCNTs linked with cysteine-capped gold nanoparticles (MWCNT-AuCys). Explanation of the calculations carried out to find the fraction of MWCNT lengths in the network that was occupied by nodes was measured. Transparency and $I-V$ plots for the MWCNT films, TEM and SEM images of the CNT networks with gold nanoparticles not capped by cysteine, TEM images of postannealed networks, and additional XPS data plots. This material is available free of charge *via* the Internet at http://pubs.acs.org.

REFERENCES AND NOTES

1. Cao, Q.; Rogers, J. A. Ultrathin Films of Single-Walled Carbon Nanotubes for Electronics and Sensors: A Review of Fundamental and Applied Aspects. *Adv. Mater.* **2009**, *21*, 29.
2. Hicks, J.; Behnam, A.; Ural, A. Resistivity in Percolation Networks of One-Dimensional Elements with a Length Distribution. *Phys. Rev. E* **2009**, *79*, 012102-4.
3. Behnem, A.; Ashkan, U. Computational Study of Geometry-Dependent Resistivity Scaling in Single-Walled Carbon Nanotube Films. *Phys. Rev. B* **2007**, *75*, 125432/1.
4. Khoo, K. H.; Chelikowsky, J. R. Electron Transport Across Carbon Nanotube Junctions Decorated with Au Nanoparticles: Density Functional Calculations. *Phys. Rev. B* **2009**, *79*, 205422.
5. Berhan, L.; Sastry, A. M. On Modeling Bonds in Fused, Porous Networks: 3D Simulations of Fibrous-Particulate Joints. *J. Compos. Mater.* **2003**, *37*, 715.
6. Berhan, L.; Yi, Y. B.; Sastry, A. M.; Munoz, E.; Selvidge, M.; Baughman, R. Mechanical Properties of Nanotube Sheets: Alterations in Joint Morphology and Achievable Moduli in Manufacturable Materials. *J. Appl. Phys.* **2004**, *95*, 4335.
7. Yu, M.; Lourie, O.; Dyer, M. J.; Moloni, K.; Kelly, T. F.; Ruoff, R. S. Strength and Breaking Mechanism of Multiwalled Carbon Nanotubes under Tensile Load. *Science* **2000**, *287*, 637.
8. Gruner, G. Carbon Nanotube Films for Transparent and Plastic Electronics. *J. Mater. Chem.* **2006**, *16*, 3533.
9. Gruner, G. Carbon Nanonets Spark New Electronics. *Sci. Am.* **2007**, 76.
10. Kong, B.-S.; Jung, D.-H.; Oh, S.-K.; Han, C.-S.; Jung, H.-T. Single-Walled Carbon Nanotube Gold Nanohybrids: Application in Highly Effective Transparent and Conductive Films. *J. Phys. Chem. C* **2007**, *111*, 8377.
11. Yu, S.; Ruizhi, Y.; Yuet, P. K. Easy Decoration of Carbon Nanotubes with Well Dispersed Gold Nanoparticles and the Use of the Material as an Electrocatalyst. *Carbon* **2009**, *47*, 1146.
12. Zhenyu, L.; Lizhang, H.; Yan, L.; Jin-Ming, L.; Yuwu, C.; Guonan, C. Electrochemiluminescent Biosensor Based on Multi-wall Carbon Nanotube/Nano-Au Modified Electrode. *Electrochem. Commun.* **2008**, *10*, 1708.
13. Lawson, G.; Gonzaga, F.; Julia, H.; de Silveira, G.; Brook, M. A.; Adronov, A. Au−Carbon Nanotube Composites from Self-Reduction of Au^{3+} upon Poly(ethylene imine) Functionalized SWNT Thin Films. *J. Mater. Chem.* **2008**, *18*, 1694.
14. Oliveira, M. M.; Zarbin, A. J. G. Carbon Nanotubes Decorated with Both Gold Nanoparticles and Polythiophene. *J. Phys. Chem. C* **2008**, *112*, 18783.
15. Kumar, N. A.; Kim, S. H.; Kim, J. S.; Kim, J. T.; Jeong, Y. T. Functionalization of Multiwalled Carbon Nanotubes with Cysteamine for the Construction of CNT/Gold Nanoparticle Hybrid Nanostructures. *Surf. Rev. Lett.* **2009**, *16*, 487.
16. Rabbani, M. M.; Chang Hyun, K.; Jong-Seong, B.; Jeong Hyun, Y.; Il Soo, K.; Weontae, O. Comparison of Some Gold/Carbon Nanotube Composites Prepared by Control of Electrostatic Interaction. *Colloids Surf. A* **2009**, *336*, 183.
17. Gingery, D.; Buhlmann, P. Formation of Gold Nanoparticles on Multiwalled Carbon Nanotubes by Thermal Evaporation. *Carbon* **2008**, *46*, 1966.
18. Qingling, H.; Maschmann, M. R.; Fisher, T. S.; Janes, D. B. Assemblies of Carbon Nanotubes and Unencapsulated Sub-10-nm Gold Nanoparticles. *Small* **2007**, *3*, 1266.
19. Kwang-Pill, L.; Showkat, A. M.; Iyengar Gopalan, A. I.; Seong-Ho, C.; Young Chang, N. Dispersion of Gold Nanoparticles into Thiol-Functionalized Carbon Nanotubes by γ-Radiation. *Diamond Relat. Mater.* **2007**, *16*, 1688.
20. Zhang, Y.; Franklin, N. W.; Chen, R. J.; Dai, H. Metal Coating on Suspended Carbon Nanotubes and Its Implication to Metal-Tube Interaction. *Chem. Phys. Lett.* **2000**, *331*, 35.
21. Mollgin, K.; Zheng, Z.; Piazzon, N. Thermal Stability and Reconstruction of Nanoparticulate Au Film on Model Molecular Surfaces. *J. Colloid Interface Sci.* **2009**, *333*, 719.
22. Yablokov, V. A.; Vasina Ya., A.; Zelyaev, I. A.; Mitrofanova, S. V. Kinetics of Thermal Decomposition of Sulfur-Containing Amino Acids. *Russ. J. Gen. Chem.* **2009**, *79*, 1141.
23. Ganesh, K. J.; Kawasaki, M.; Zhou, J. P.; Ferreira, P. J. A STEM Parallel Diffraction Technique Applied to Nanomaterials. *Microsc. Microanal.* **2009**, *15*, 752.
24. Ganesh, K. J.; Kawasaki, M.; Zhou, J. P.; Ferreira, P. J. In review Microscopy and Microanalysis.
25. Briggs, D. *Handbook of X-ray and Ultraviolet Photoelectron Spectroscopy*; Hayden and Son Ltd.: London, 1978.
26. Briggs, D.; Seah, M. P. *Practical Surface Analysis: Auger and X-ray Photoelectron Spectroscopy*; John Wiley and Sons: New York, 1996; Vol. I.
27. Castner, D. G.; Hinds, K.; Grainger, D. W. X-ray Photoelectron Spectroscopy Sulfur 2p Study of Organic Thiol and Disulfide Binding Interactions with Gold Surfaces. *Langmuir* **1996**, *12*, 5083.
28. Cavalleri, O.; Gonella, G.; Terreni, S.; Vignolo, M.; Pelori, P.; Floreano, L.; Morgante, A.; Canepa, M.; Rolandi, R. High Resolution XPS of the S 2p Core Level Region of the L-Cysteine/gold Interface. *J. Phys.: Condens. Matter* **2004**, *16*, S2477.
29. Dodero, G.; De Michieli, L.; Cavalleri, O.; Rolandi, R.; Oliveri, L.; Dacca, A.; Parodi, R. L- Cysteine Chemisorption on Gold an XPS and STM Study. *Colloids Surf. A* **2000**, *175*, 121.
30. Yablokov, V. A.; Vasina, Ya. A.; Zelyaev, I. A.; Mitrofanova, S. V. Kinetics of Thermal Decomposition of Sulfur-Containing Amino Acids. *Russ. J. Gen. Chem.* **2009**, *79*, 1141.
31. Benayad, A.; Shin, H.-J.; Park, H.-k.; Yoon, S.-M.; Kim, K. K.; Jin, M. H.; Jeong, H.-K.; Lee, J. C.; Choi, J. Y.; Lee, Y.-H. Controlling Work Function of Reduced Graphite Oxide with Au-Ion Concentration. *Chem. Phys. Lett.* **2009**, *475*, 91.
32. XPS Studies of Supported Gold Catalysts the Role of Au^{0} and $Au^{\delta+}$ Species as Active Sites. *Surf. Interface Anal.* **2006**, *38*, 215.
33. van der Pauw, L. J. A Method of Measuring the Resistivity and Hall Coefficient on Lamellae of Arbitrary Shape. *Philips Technical Review* **1958**, *20*, 220.
34. Ruoff, R. Method and System for Improving Conductivity and Mechanical Performance of Carbon Nanotube Nets and Related Materials. Patent Application #20090155460, 2009.
35. Rodríguez-Manzo, J. A.; Wang, M.-S.; Banhart, F.; Bando, Y.; Golberg, D. Multibranched Junctions of Carbon Nanotubes *via* Cobalt Particles. *Adv. Mater.* **2009**, *21*, 4477.
36. Ramanathan, T.; Fisher, F. T.; Ruoff, R. S.; Brinson, L. C. Amino-Functionalized Carbon Nanotubes for Binding to Polymers and Biological Systems. *Chem. Mater.* **2005**, *17*, 1290.
37. Hak Yong, K.; Aryal, S.; Remant, B. K. C.; Dharmaraj, N.; Bhattarai, N.; Chi Hun, K. Spectroscopic Identification of S−Au Interaction in Cysteine Capped Gold Nanoparticles. *Spectrochim. Acta, Part A* **2006**, *63*, 160.
38. Wu, Z.; Chen, Z.; Du, X.; Logan, J. M.; Sippel, J.; Nikolou, M.; Kamaras, K.; Reynolds, J. R.; Tanner, D. B.; Hebard, A. F.; Rinzler, A. G. Transparent, Conductive Carbon Nanotube Films. *Science* **2004**, *305*, 1273.